Electronic Supplementary Material (ESI) for Sustainable Energy & Fuels.

Electronic Supplementary Information

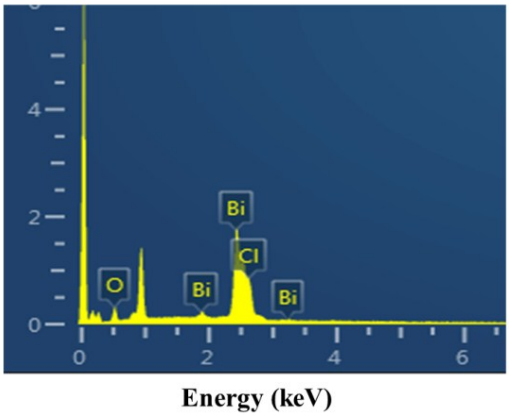

Fig. S1 EDX spectrum of the BiOCl NPs.

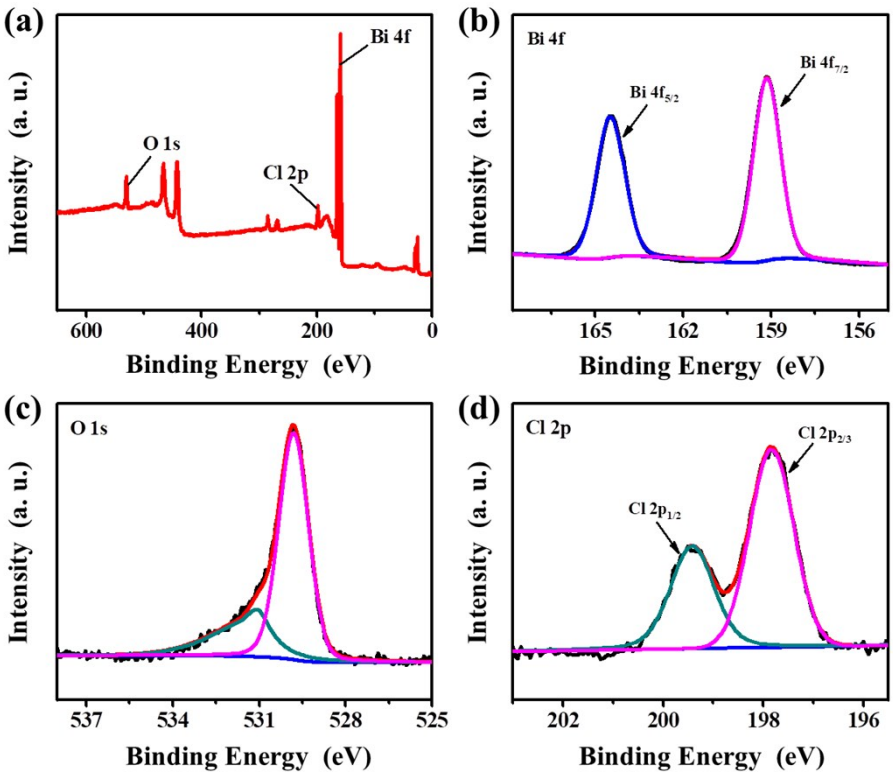

Fig. S2 (a) XPS survey spectrum of the BiOCl NPs. (b) Bi 4f, (c) O 1s and (d) Cl 2p XPS high-resolution spectra of the BiOCl NPs.

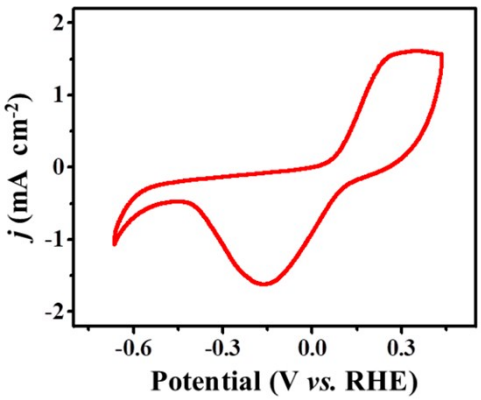

Fig. S3 CV curve of BiOCl NPs showing the in situ electrochemical reduction from BiOCl to Bi at cathodic potentials. The CV curve was recorded at a scan rate of 10 mV s^{-1}.

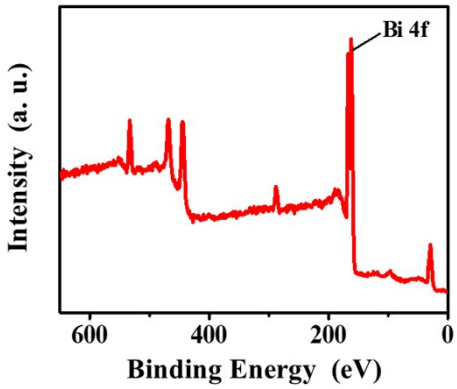

Fig. S4 XPS survey spectrum of the Bi NSs.

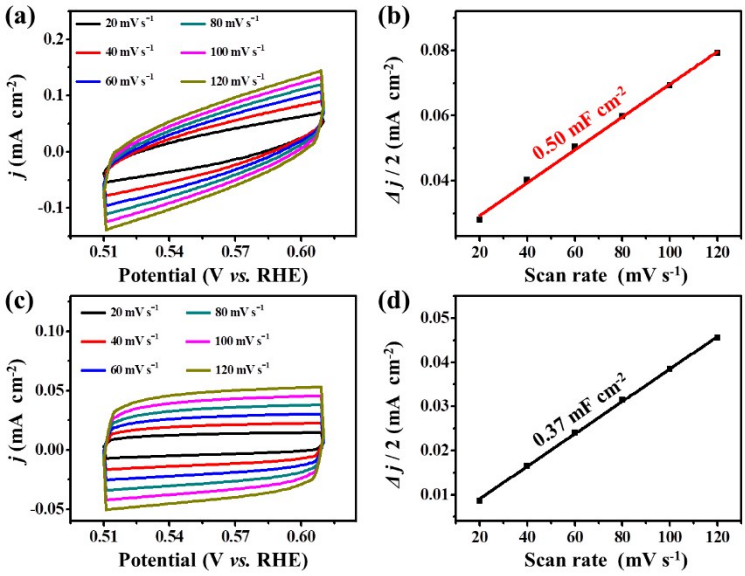

Fig. S5 The CV curves at various scan rates (20 to 120 mV s^{-1}) and capacitive current densities of (a,b) Bi NSs, (c,d) BiOCl NPs in 0.1 M Na_2SO_4 aqueous solution.

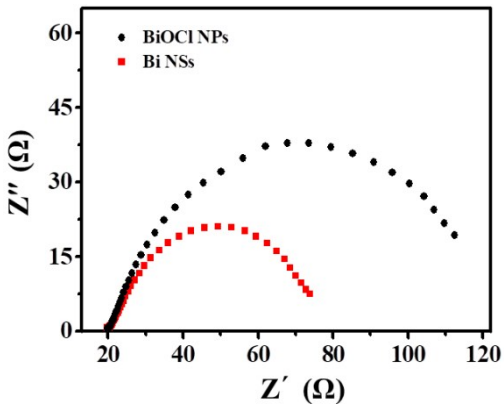

Fig. S6 Electrochemical impedance spectra of BiOCl NPs and Bi NSs at -1.0 V.

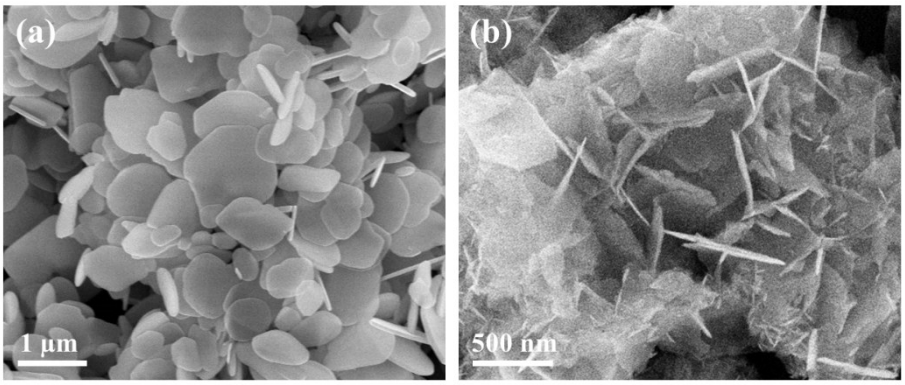

Fig. S7 SEM images of (a) BiOBr nanoplates and (b) Bi nanosheets obtained from the BiOBr nanoplate precursors.

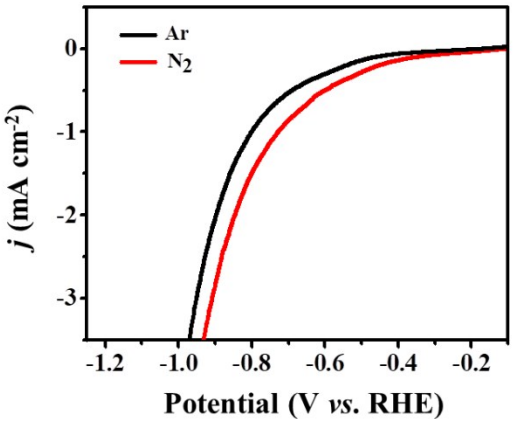

Fig. S8 LSV curves of the Bi NSs in Ar-saturated and N_2-saturated 0.1 M Na_2SO_4 aqueous solution, respectively.

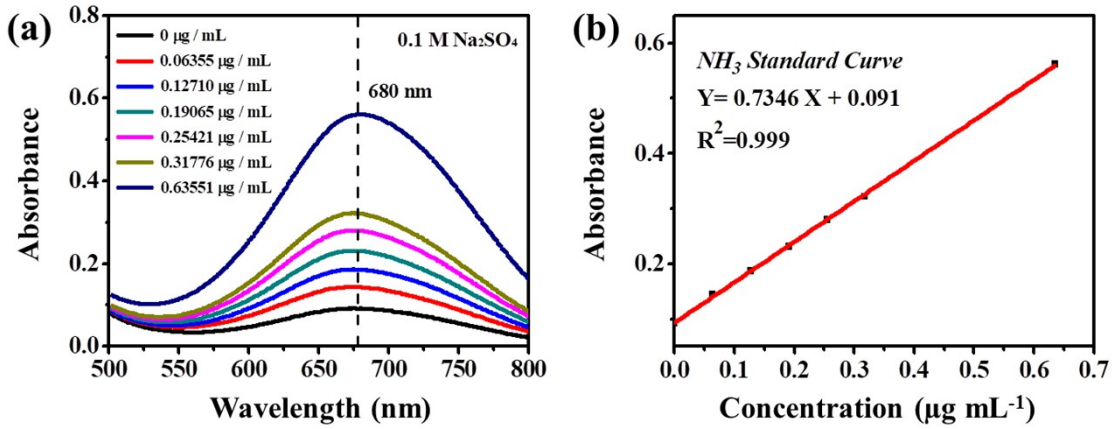

Fig. S9 (a) UV−vis absorption spectroscopy of various NH_4^+ ions concentrations with the indophenol indicator for 2 h at room temperature. (b) Calibration curve used to estimate the concentrations of NH_3 by NH_4^+ ion concentration.

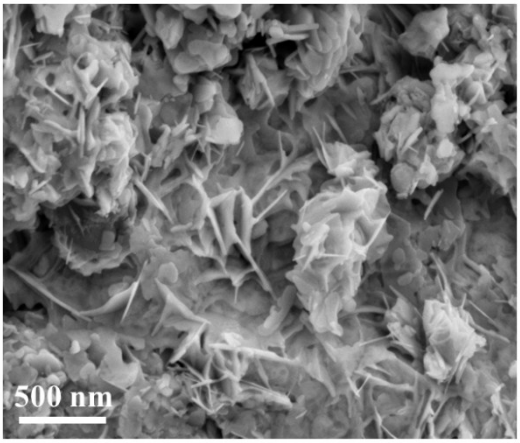

Fig. S10 SEM image of commercial Bi.

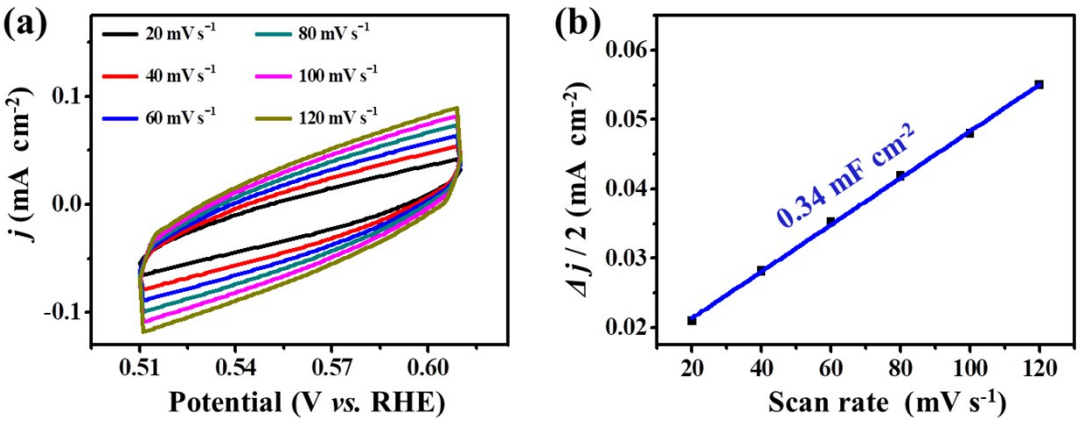

Fig. S11 (a) The CV curves at various scan rates and (b) capacitive current densities of commercial Bi in 0.1 M Na_2SO_4 aqueous solution.

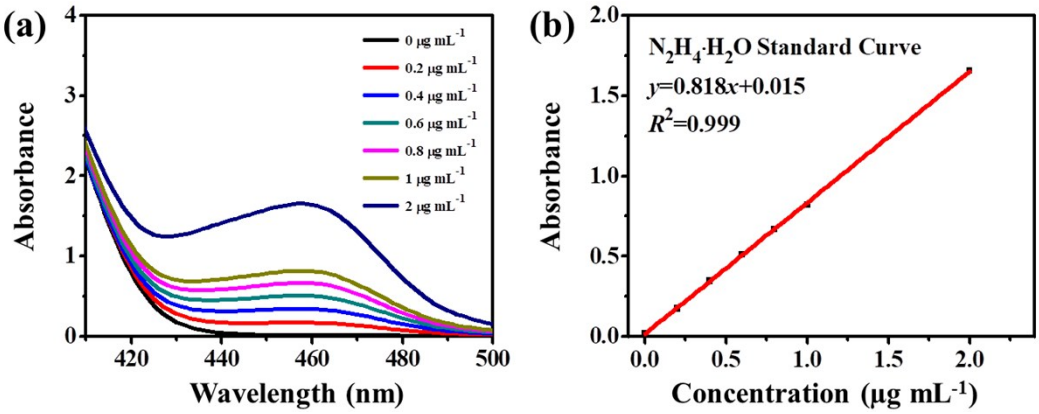

Fig. S12 (a) UV−vis absorption spectroscopy of various $N_2H_4 \cdot H_2O$ concentrations with the indicator for 15 min at room temperature. (b) The calibration curve used for estimation of N_2H_4 concentration.

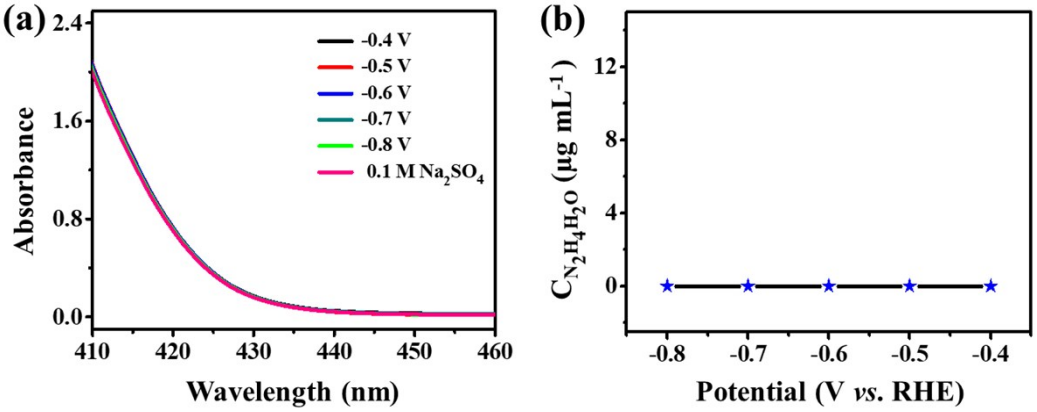

Fig. S13 (a) UV−vis absorption spectra and (b) The $N_2H_4 \cdot H_2O$ concentration of the electrolysis with the indicator for 20 min after charging at a series of potentials for 2 h using Bi NSs as electrocatalysts.

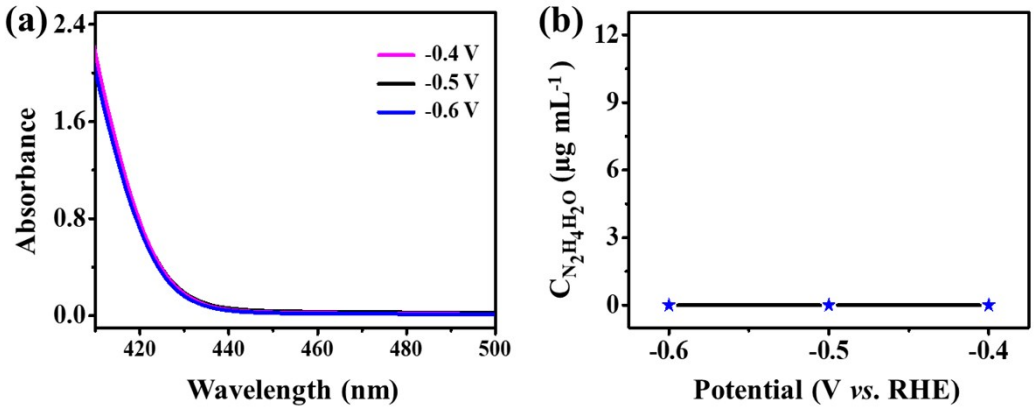

Fig. S14 (a) UV−vis absorption spectra and (b) The $N_2H_4 \cdot H_2O$ concentration of the electrolysis with the indicator for 20 min after charging at a series of potentials for 2 h using commercial Bi powder as electrocatalysts.

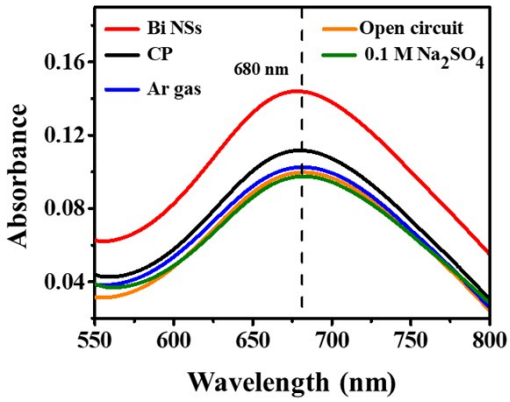

Fig. S15 UV−vis absorption spectroscopy of the electrolytes stained with the indophenol indicator under different conditions.

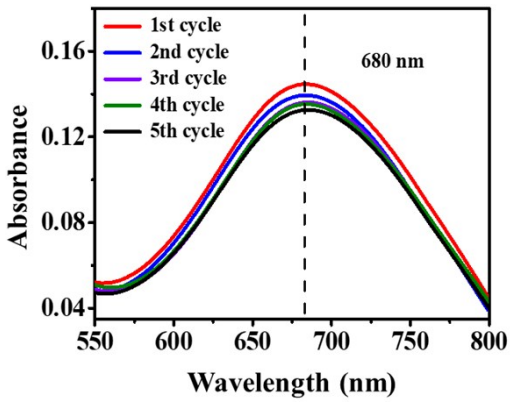

Fig. S16 UV−vis absorption spectroscopy of the electrolytes stained with the indophenol indicator after different cycles.

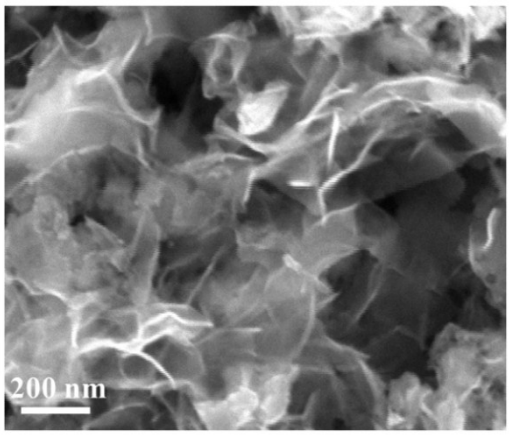

Fig. S17 SEM image of Bi NSs after electrocatalytic stability testing.

Table S1. Performance comparison between the as-prepared Bi NSs and some other reported electrocatalysts in Na_2SO_4 solutions.

Electrocatalysts	Electrolytes	NH_3 yield	FE(%)	Ref.
Bi NSs	**0.1 M Na_2SO_4**	**11.11 μg h^{-1} $mg^{-1}_{cat.}$ (4.48 μg h^{-1} cm^{-2})**	**14.14**	**This work**
Plasma R-O-Bi	0.2 M Na_2SO_4	5.453 μg h^{-1} $mg^{-1}_{cat.}$	11.68	1
$BiVO_4$	0.2 M Na_2SO_4	8.60 μg h^{-1} $mg^{-1}_{cat.}$	10.04	2
BD-Ag/AF	0.1 M Na_2SO_4	2.68 μg h^{-1} cm^{-2}	7.36	3
MoS_2/CC	0.1 M Na_2SO_4	4.94 μg h^{-1} $mg^{-1}_{cat.}$	1.17	4
V_2O_3/C	0.1 M Na_2SO_4	2.46 μg h^{-1} cm^{-2}	7.28	5
Fe_3O_4/Ti	0.1 M Na_2SO_4	3.43 μg h^{-1} cm^{-2}	2.6	6
MnO/TM	0.1 M Na_2SO_4	7.92 μg h^{-1} $mg^{-1}_{cat.}$	8.02	7
d-FG/CP	0.1 M Na_2SO_4	9.3 μg h^{-1} $mg^{-1}_{cat.}$	4.2	8
8YSZ	0.1 M Na_2SO_4	10.84 μg h^{-1} $mg^{-1}_{cat.}$	12.3	9
SnO_2/CC	0.1 M Na_2SO_4	4.03 μg h^{-1} $mg^{-1}_{cat.}$	2.17	10
FeS@MoS_2/CFC	0.1 M Na_2SO_4	6.34 μg h^{-1} $mg^{-1}_{cat.}$	2.96	11
AuNPs@MoS_2	0.1 M Na_2SO_4	5.65 μg h^{-1} $mg^{-1}_{cat.}$	9.7	12
S−Bi nanobelt	0.1 M Na_2SO_4	10.28 μg h^{-1} $mg^{-1}_{cat.}$	10.48	13

References

[1] Y. Wang, M.-m. Shi, D. Bao, F.-l. Meng, Q. Zhang, Y.-t. Zhou, K.-h. Liu, Y. Zhang, J.-z. Wang, Z.-w. Chen, D.-p. Liu, Z. Jiang, M. Luo, L. Gu, Q.-h. Zhang, X.-z. Cao, Y. Yao, M.-h. Shao, Y. Zhang, X.-B. Zhang, J. G. Chen, J.-m. Yan and Q. Jiang, *Angew. Chem. Int. Ed.*, 2019, **58**, 9464-9469.

[2] J. X. Yao, D. Bao, Q. Zhang, M. M. Shi, Y. Wang, R. Gao, J. M. Yan and Q. Jiang, *Small Methods*, 2018, **3**, 1800333.

[3] L. Ji, X. Shi, A. M. Asiri, B. Zheng and X. Sun, *Inorg. Chem.*, 2018, **57**, 14692-14697.

[4] L. Zhang, X. Ji, X. Ren, Y. Ma, X. Shi, Z. Tian, A. M. Asiri, L. Chen, B. Tang and X. Sun, *Adv. Mater.*, 2018, **30**, 1800191.

[5] R. Zhang, J. Han, B. Zheng, X. Shi, A. M. Asiri and X. Sun, *Inorg. Chem. Front.*, 2019, **6**, 391-395.

[6] Q. Liu, X. Zhang, B. Zhang, Y. Luo, G. Cui, F. Xie and X. Sun, *Nanoscale*, 2018, **10**, 14386-14389.

[7] Z. Wang, F. Gong, L. Zhang, R. Wang, L. Ji, Q. Liu, Y. Luo, H. Guo, Y. Li, P. Gao, X. Shi, B. Li, B. Tang and X. Sun, *Adv. Sci.*, 2019, **6**, 1801182.

[8] J. Zhao, J. Yang, L. Ji, H. Wang, H. Chen, Z. Niu, Q. Liu, T. Li, G. Cui and X. Sun, *Chem. Commun.*, 2019, **55**, 4266-4269.

[9] H. Xian, Q. Wang, G. Yu, H. Wang, Y. Li, Y. Wang and T. Li, *Applied Catalysis A: General*, 2019, **581**, 116-122.

[10] L. Zhang, X. Ren, Y. Luo, X. Shi, A. M. Asiri, T. Li and X. Sun, *Chem. Commun.*, 2018, **54**, 12966-12969.

[11] Y. Guo, Z. Yao, B. J. J. Timmer, X. Sheng, L. Fan, Y. Li, F. Zhang and L. Sun, *Nano Energy*, 2019, **62**, 282-288.

[12] Y. Zhou, X. Yu, X. Wang, C. Chen, S. Wang and J. Zhang, *Electrochimica Acta*, 2019, **317**, 34-41.

[13] Y. Lin, L. Yang, H. Jiang, Y. Zhang, Y. Bo, P. Liu, S. Chen, B. Xiang, G. Li, J. Jiang, Y. Xiong and L. Song, *J. Phys. Chem. Lett.*, 2020, **11**, 1746-1752.